MTL TR 92-50

AD

EQUIBIAXIAL TESTING OF TP-14AX CARBON BLACK RUBBER SHEETS

ROBERT P. BAMBERG, RONALD P. AGHABABIAN,
CHRISTOPHER CAVALLARO, and ARTHUR R. JOHNSON
MECHANICS AND STRUCTURES BRANCH

August 1992

Approved for public release; distribution unlimited.

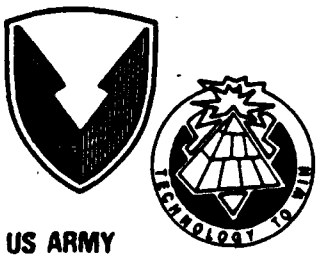

US ARMY
LABORATORY COMMAND
MATERIALS TECHNOLOGY LABORATORY

U.S. ARMY MATERIALS TECHNOLOGY LABORATORY
Watertown, Massachusetts 02172-0001

The findings in this report are not to be construed as an official Department of the Army position, unless so designated by other authorized documents.

Mention of any trade names or manufacturers in this report shall not be construed as advertising nor as an official indorsement or approval of such products or companies by the United States Government.

DISPOSITION INSTRUCTIONS

Destroy this report when it is no longer needed.
Do not return it to the originator

UNCLASSIFIED

SECURITY CLASSIFICATION OF THIS PAGE *(When Data Entered)*

REPORT DOCUMENTATION PAGE		READ INSTRUCTIONS BEFORE COMPLETING FORM
1. REPORT NUMBER MTL TR 92-50	2. GOVT ACCESSION NO.	3. RECIPIENT'S CATALOG NUMBER
4. TITLE *(and Subtitle)* EQUIBIAXIAL TESTING OF TP-14AX CARBON BLACK RUBBER SHEETS		5. TYPE OF REPORT & PERIOD COVERED Final Report 6. PERFORMING ORG. REPORT NUMBER
7. AUTHOR(s) Robert P. Bamberg, Ronald R. Aghababian, Christopher Cavallaro, and Arthur R. Johnson		8. CONTRACT OR GRANT NUMBER(s)
9. PERFORMING ORGANIZATION NAME AND ADDRESS U.S. Army Materials Technology Laboratory Watertown, Massachusetts 02172-0001 SLCMT-MRS		10. PROGRAM ELEMENT, PROJECT, TASK AREA & WORK UNIT NUMBERS D/A Project: 1L161102AH42
11. CONTROLLING OFFICE NAME AND ADDRESS U.S. Army Laboratory Command 2800 Powder Mill Road Adelphi, Maryland 20783-1145		12. REPORT DATE August 1992 13. NUMBER OF PAGES 38
14. MONITORING AGENCY NAME & ADDRESS *(if different from Controlling Office)*		15. SECURITY CLASS. *(of this report)* Unclassified 15a. DECLASSIFICATION/DOWNGRADING SCHEDULE
16. DISTRIBUTION STATEMENT *(of this Report)* Approved for public release; distribution unlimited.		
17. DISTRIBUTION STATEMENT *(of the abstract entered in Block 20, if different from Report)*		
18. SUPPLEMENTARY NOTES		
19. KEY WORDS *(Continue on reverse side if necessary and identify by block number)* Elastomers Inflation tests Stress-stretch tests		
20. ABSTRACT *(Continue on reverse side if necessary and identify by block number)* (SEE REVERSE SIDE)		

DD FORM 1 JAN 73 1473 EDITION OF 1 NOV 65 IS OBSOLETE

UNCLASSIFIED

SECURITY CLASSIFICATION OF THIS PAGE *(When Data Entered)*

Block No. 20

ABSTRACT

The classical inflation test for thin rubber disks was used to obtain equibiaxial stress-stretch data for a carbon black filled rubber (TP-14AX). Details of the experimental setup, test procedure, measured data, and material constants obtained from the data are reported. A review of how to use the measured test data with tensile stress-stretch data to obtain the material constants is presented. Complete results (data to material constants) for three test specimens are reported.

CONTENTS

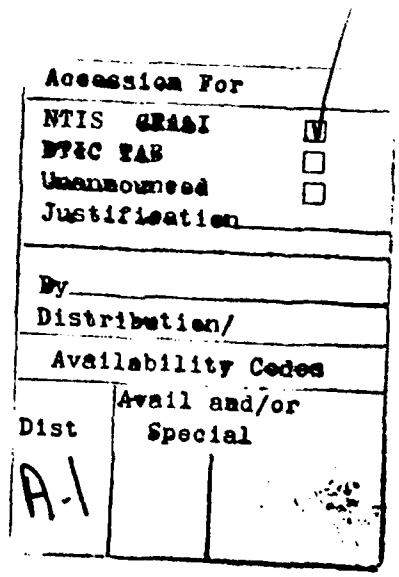

INTRODUCTION

A classical test method developed to determine equibiaxial stress-stretch data for large deformations of incompressible membranes is used in this effort to obtain data for TP-14AX carbon black filled rubber sheets. The method requires that flat membranes be inflated through a circular hole to create an axisymmetric balloon shape, the apex of which is approximately spherical. In this case, for an incompressible material, explicit relations exist between the pressure, radius of curvature at the apex, undeformed thickness of the membrane, and derivatives of the material's energy density function. Given the pressure, radius of curvature, and initial thickness data for an inflation test, least squares methods can be used to determine the material constants in the energy density function by selecting them so that the explicit relation mentioned above best fits the data. This report is part of a larger effort where models are being developed for general states of stress for both static and viscoelastic deformations of rubberlike materials. The purpose of this report is to document the results of the membrane inflation experiment. A demonstration is also provided of how the data is used by selecting an energy density function and determining its constants using the method of minimization of least squares with a constraint. It is noted with the exception of a few special materials a single test is not sufficient to determine an energy function which would be useful for general deformations. Thus, in the demonstration the biaxial data measured in this effort was combined with some previously determined uniaxial tension data to determine a strain energy density function for the material.

The inflation test is described by Treloar[1] and Rivlin and Saunders[2] in their studies of rubber. In this effort, square flat rubber sheets were clamped in a special jig which had a circular hole on one side and attachments for supplying air pressure on the other side. The disk of rubber covering the circular hole of the jig was then inflated to form a bubble. The top of the bubble was approximately spherical. Its image was projected onto (and marked on) graph paper. Calibration of the projection process then allowed for approximate radii of curvature of the inflated bubbles and the deformed arc lengths between marked points to be determined. The undeformed geometry, deformed geometry and pressure were then used to determine the biaxial stress versus stretch ratio data. Details of the experimental setup, material tested, calibration process, jig design, measured data, computed stress versus stretch ratio data, and the method for determining material constants are presented.

MATERIAL DESCRIPTION

The square rubber tensile sheets tested were prepared for the U.S. Army Materials Technology Laboratory (MTL) in 1987 by the U.S. Army Belvoir Research and Development Center. The samples used in this effort had been stored at room temperature at MTL since they arrived in 1987. The tests were conducted from July 1990 to September 1990. The sheets were prepared according to ASTM D3182-87. The mold dimensions for the membrane were 6 x 6 x 0.08 in. The actual thickness of each sheet was determined at the end of each test. The material designation is TP-14AX, a triblend of natural rubber, SBR, and Takatene, as described in Table 1. Typical properties for TP-14AX are listed in the Appendix.

1. TRELOAR, L. R. G. *Stress-Strain Data for Vulcanized Rubber Under Various Types of Deformation*. Trans. Faraday Soc., v. 40, 1944, p. 59-70.
2. RIVLIN, R. S., and SAUNDERS, D. W. *Large Elastic Deformations of Isotropic Materials. VII. Experiments on the Deformation of Rubber*. Phil. Trans. R. Soc., v. 243, 1951, p. 251-288.

EXPERIMENTAL SETUP AND JIG DESIGN

In order to obtain a sharp calibrated shadow image of the inflated membrane a Bausch & Lomb™ projection lamp was positioned on a table 6 feet 6 inches away from the midpoint of the test specimen. A large sheet of graph paper was then positioned 2 feet 6 inches away from the opposite side of the specimen region making the total distance between lamp and graph paper 9 feet (see Figure 1).

The specimen itself was sandwiched in a jig that was bolted to an Instron™ machine surrounded by plexiglass shields. The jig consists of two aluminum plates, a clamping ring, and four fixture supports. The top aluminum plate has a 3-inch-diameter hole in the center (see Figures 2 and 3). Surrounding the hole, on the underside of the top plate, is a circular raised lip or clamping ring (see Figure 4). This ring, along with the cut groove in the bottom aluminum plate, adequately stops slippage of the specimen and leakage of air pressure when the plates are bolted together (see Figures 5 through 7). Within the circumference of the bottom plate's groove are three threaded holes used for regulating air pressure (see Figure 8). The center hole was used as the compressed air inlet. A second hole to the right of the inlet was used for an air outlet valve. The third had a pressure transducer attached to monitor the air pressure inside the inflated rubber shell. The four fixture supports were attached to the bottom plate which provided enough room for the pipes, gauges, and valves needed to control the pressure (see Figure 9).

A compressor supplied air to one end of a pipe system which consisted of two valves separated by a pressure gauge. The other end of the pipe system was connected to the center hole of the bottom plate. The gauge was positioned between both valves so that it could measure either the pressure on the compressor side or on the specimen side depending upon which valves were left open (see Figure 10). First valve open and second valve closed increases the pressure acting on the membrane; inversely, first valve closed and second valve open would measure pressure inflating the rubber specimen. Both valves open allows the air from the compressor to directly inflate the specimen. The graph paper was set up so that the specimen's shadow would fall completely onto it for the entire range of pressures used in the test.

CALIBRATION OF THE IMAGE

The geometrical relationship between the image of the specimen cast on the graph paper and the specimen's cross-sectional dimensions was approximated with a bilinear scaling function. The coefficients were determined by measuring the images of flat rectangular gauged specimens (see Figure 11); i.e., a mapping of the form

$$x = \alpha_1 + \alpha_2 X + \alpha_3 Y + \alpha_4 XY$$
$$y = \beta_1 + \beta_2 X + \beta_3 Y + \beta_4 XY \qquad (1)$$

was assumed where (x,y) are the coordinates of a point in the specimen's midplane and (X,Y) are its coordinates on the image plane (graph paper).

It should be noted that the image cast by the inflated rubber sheet does not come exactly from its midplane; i.e., the light rays from the *point source* which are tangent to the sphere produce a larger image than the actual midplane semicircle image should be.

However, a calculation of the error for this geometrical effect indicates the error in predicting the actual location is less than 0.3% given the dimensions of the experimental setup.

The data shown in Table 2 was used to make the following least squares approximation to Equation 1:

$$x = (-0.02949) + (0.7245)X + (0.01028)Y + (-0.002077)XY$$
$$y = (0.03594) + (-0.006263)X + (0.7345)Y + (0.002508)XY \quad (2)$$

Table 3 then compares the actual measured values for the three cutouts to their computed values using the scaling function given by Equation 2.

EXPERIMENTAL PROCEDURE

Each specimen was cyclically strained prior to recording data to remove nonrepeatable effects which occur when virgin rubberlike materials are deformed.[3] This was done by cycling; i.e., inflating/deflating, the rubber sheet from 0 psi to approximately 30 psi 20 times. The specimen was then left for a period of no less than two hours in its inflated deformed shape. Next, it was deflated and marked with three points along its centerline (perpendicular to the rays from the light source). The image of the specimen and the three points were then recorded at the pressure of 0 psi. It is noted that the marks on each specimen were not made at any particular distance apart from one another since they were needed only to track the growth of the sphere as the pressure was incremented.

The sheet was then inflated to 10 psi and held inflated at that pressure for 10 minutes. After the 10 minute period, the image was traced on the graph paper along with the corresponding three points associated with the marks (see Figure 12). These points were recorded by marking the intersecting shadows of the rubber specimen and of a pointer which was touching the marked point on the specimen. The pressure was recorded next to the specimen's image.

The rubber specimen was incrementally inflated from 10 psi to 55 psi in 5 psi increments while repeating the above mentioned procedure. Ten data points were recorded (10 pressure values) for each of the three marks on the membrane (see Tables 4 through 6 for the recorded data). During the 10 minute wait period after each pressure increment the pressure would drop due to leaks and because the pressurized volume was increasing due to creep. During the time required to mark the data points on the graph paper there was no noticeable change in pressure. In addition, the shape of the apex region of the rubber sheet appeared spherical throughout the entire test. When all the tests were completed, the marked points on the graph paper were measured using a vernier caliper. Each shadow point was then converted to its actual size by use of the calibration Equation 2.

The maximum pressure of 55 psi was chosen because one of the TP-14AX carbon black rubber sheets ruptured slightly beyond it. Figure 13 shows photos of a relaxed deformed specimen after testing, as well as the failed test specimen. It is noted that the failure occurred at the apex and the relaxed deformed shape is symmetrical.

3. MULLINS, L. *Softening of Rubber by Deformation.* Rubber Chemistry and Technology, v. 42, 1969, p. 339-362.

MATERIAL CONSTANTS

The stress-strain response of rubber, without consideration of viscoelastic effects, is modeled with strain energy density functions.[4] There are numerous algebraic forms available for the energy function. Typically, these functions are represented by expansions in powers of the strain invariants or stretch ratios. In this effort the least squares minimization procedure for Rivlin energy functions as described by James, Green, and Simpson[5] and modified by Johnson, et al.[6] was followed. The method is described in Equation 3. Consider a Rivlin energy function of the form

$$W = \sum_{\ell+m}^{3} \sum_{\geq 1}^{3} C_{\ell m} (I_1 - 3)^{\ell} (I_2 - 3)^{m} \tag{3}$$

where

$$I_1 = \lambda_1^2 + \lambda_2^2 + \lambda_3^2$$

and

$$I_2 = 1/\lambda_1^2 + 1/\lambda_2^2 + 1/\lambda_3^2 .$$

The quantities I_1 and I_2 are invariants of the deformation and λ_1, λ_2, and λ_3 are the principal stretch ratios. The coefficients $C_{\ell m}$ are typically computed by the following test and least squares fitting procedure.[5] The engineering stresses for uniaxial tension and shear, and for equibiaxial tension computed using Equation 1 (σ^T, σ^S, and σ^B, respectively) are

$$\sigma^{*} = \sum_{\ell+m}^{3} \sum_{\geq 1}^{3} C_{\ell m} A^{*}_{\ell m} \tag{4}$$

where

$* = T, S, \text{ or } B,$

$$A^{T}_{\ell m} = 2\left[\lambda - \frac{1}{\lambda^2}\right]\left[\ell (I_1 - 3)^{\ell-1} (I_2 - 3)^{m} + \frac{m}{\lambda} (I_1 - 3)^{\ell} (I_2 - 3)^{m-1}\right] \tag{5}$$

$$A^{S}_{\ell m} = 2\left[\lambda - \frac{1}{\lambda^3}\right]\left[\ell (I_1 - 3)^{\ell-1} (I_2 - 3)^{m} + m (I_1 - 3)^{\ell} (I_2 - 3)^{m-1}\right] \tag{6}$$

$$A^{B}_{\ell m} = 2\left[\lambda - \frac{1}{\lambda^5}\right]\left[\ell (I_1 - 3)^{\ell-1} (I_2 - 3)^{m} + m\lambda^2 (I_1 - 3)^{\ell} (I_2 - 3)^{m-1}\right] \tag{7}$$

4. TRELOAR, L. R. G. *The Physics of Rubber Elasticity.* Clarendon Press, United Kingdom, 1975.
5. JAMES, A. G., GREEN, A., and SIMPSON, G. M. *Strain Energy Functions of Rubber. I. Characterizations of Gum Vulcanizates.* J. Appl. Pol., Sc., v. 19, 1975, p. 2033-2058.
6. JOHNSON, A. R., QUIGLEY, C. J., COX, D. L., BISSONNETTE, L. C., and MACIEJEWSKI, W. C. *Constitutive Coefficients for Viscohyperelastic Materials.* Transactions of the Ninth Army Conference on Applied Mathematics and Computing, U.S. Army Research Office, 1992.

and λ = the stretch ratio measured in the direction of loading; i.e., the extensional stretch (see Reference 5). The invariants for tension are given by

$$I_1 = \lambda^2 + 2/\lambda \text{ and } I_2 = 2\lambda + 1/\lambda^2 \tag{8}$$

for shear by

$$I_1 = I_2 = 1 + \lambda^2 + 1/\lambda^2 \tag{9}$$

and for equibiaxial tension by

$$I_1 = 2\lambda^2 + 1/\lambda^4 \text{ and } I_2 = 2/\lambda^2 + \lambda^4 . \tag{10}$$

An error function $\prod$ is constructed from the experimental data as follows: (* = T, S, B),

$$\prod = \sum_{*} \sum_{e} (\sigma_e^* - \sigma^* (\lambda_e))^2 \tag{11}$$

where "e" implies the measured data, σ_e^* implies the measured engineering stresses, and $\sigma^*(\lambda_e)$ implies the engineering stresses computed using the measured stretch, λ_e, in Equations 4 through 10. The constants $C_{\ell m}$ are then selected to minimize the least squares error given by Equation 11 and are computed as follows: Let

$$\{A_e^*\}^T = \{A_{10}^* (\lambda_e), A_{01}^* (\lambda_e), \ldots , A_{03}^* (\lambda_e)\} \tag{12}$$

and

$$\{C\}^T = \{C_{10}, C_{01}, \ldots , C_{03}\} . \tag{13}$$

Then, Equation 11 becomes

$$\prod = \text{constant} - 2 \sum_{*} \sum_{e} \sigma_e^* \{A^* (\lambda_e)\}^T \{C\} + \{C\}^T \left(\sum_{*} \sum_{e} \{A^* (\lambda_e)\} \{A^* (\lambda_e)\}^T \right) \{C\} \tag{14}$$

Let

$$\{b\}^T = \sum_{*} \sum_{e} \sigma_e^* \{A^* (\lambda_e)\}^T \tag{15}$$

and

$$[A] = \sum_{*} \sum_{e} \{A^* (\lambda_e) \{A^* (\lambda_e)\}^T . \tag{16}$$

Then, the least squares error function $\prod$ becomes

$$\prod = \text{constant} - 2\{b\}^T\{C\} + \{C\}^T[A]\{C\} \tag{17}$$

and the minimum error occurs when the first variation of $\prod$ is zero; i.e., when

$$\{C\} = [A]^{-1}\{b\}. \tag{18}$$

In general, both positive and negative constants are obtained from Equation 18. It was shown by Johnson, et al.[6] that the energy functions obtained by using these constants are often unstable (the functions do not obey conservation of energy requirements). It was also shown[6] that a practical remedy is to require that the constants {C} be positive when $\prod$ is minimized in Equation 17, and then to verify if energy stability constraint equations for the constants are satisfied. Thus, in this effort the constants were constrained to be larger than or equal to zero.

To prepare the inflation test equibiaxial data for the constrained least squares code the radius of curvature was first calculated for the set of three (x,y) pairs at each pressure; the geometry is shown in Figure 14. It is shown[7] as

$$R = \frac{abc}{4A} \tag{19}$$

where

$$A = \frac{1}{2}\left|\vec{V}_1 \times \vec{V}_2\right|,$$

$$\vec{V}_1 = (x_2 - x_1)\hat{i} + (y_2 - y_1)\hat{j},$$

$$\vec{V}_2 = (x_3 - x_1)\hat{i} + (y_3 - y_1)\hat{j},$$

$$a = \sqrt{(x_3 - x_2)^2 + (y_3 - y_2)^2} \qquad b = \sqrt{(x_3 - x_1)^2 + (y_3 - y_1)^2}$$

$$c = \sqrt{(x_2 - x_1)^2 + (y_2 - y_1)^2}$$

7. TUMA, Jan J. Engineering Mathematics Handbook, McGraw-Hill Book Company, New York, 1970.

With the radius of curvature, R, and the coordinates of the left and right points the arc length is given by

$$\text{Arc Length} = R\Theta \tag{20}$$

$$L = \sqrt{(x_2 - x_1)^2 + (y_2 - y_1)^2}$$

$$\Theta = 2\sin^{-1}\left(\frac{L/2}{R}\right) .$$

Then,

$$\lambda = \text{(new arc length)/(original arc length)} \tag{21}$$

Tables 7 through 9 contain the computed values for radius of curvature, angle, and arc length for each of the three tests at each of their individually held pressures. It is from these values that the measured nominal stresses for the least square fit is computed. They are given by

$$\sigma^B = \frac{PR\lambda}{2h_o} \tag{22}$$

where

P = the inflation pressure and h_o = the undeformed membrane thickness.

The stretch ratio data along with the corresponding nominal stress values for the tests are listed in Table 10 which also includes stretch-stress data from a tension test performed on the same carbon black rubber material TP-14AX on March 9, 1990. The data from this tension test was taken after the virgin rubber material had been conditioned, similarly to the way the TP-14AX carbon black rubber sheets had been worked for the inflation test.

The tensile specimen's initial length before cyclic conditioning was 4.538 inches, and had an area of 0.01862 in^2. After conditioning, the material was allowed to relax overnight. The next day, initial conditions of length and area were 4.757 and 0.01721, respectively. It was from these initial conditions that the tension stretch-stress data of Table 10 was measured.

Rivlin energy function material constants for TP-14AX carbon black rubber were found using the constrained least squares method explained above with the stretch-stress data of Table 10. The least squares fit for the experimental data are shown in Figures 16 through 18 for samples 1 through 3. Figure 19 shows the least squares fit to the experimental data of all three tests together. The material constants determined from each of the three individual least squares fits are listed in Table 11. The initial shear modulus, $G = 2(C_{10} + C_{01})$, was 163 psi, 134 psi, and 159 psi for samples 1, 2, and 3, respectively. It should be noted that the energy functions obtained from the least squares fit are stable in tensile, equibiaxial, and shear deformations.

DISCUSSION AND CONCLUSIONS

The classical inflation test for obtaining biaxial stress-stretch ratio data for rubberlike materials was performed for TP-14AX carbon black filled rubber sheets. A description of the material tested, the experimental equipment and procedure, and a demonstration of how to use the data were presented. The data obtained was useful for characterizing the energy density of TP-14AX when repeatedly deformed in an equibiaxial tensile mode. It was combined with uniaxial stress-stretch data to determine the energy density function.

It is suggested that an automated system be developed for this classical test so that equibiaxial data (which is essential for determining the energy density function used in stress analyses) can be obtained quickly and accurately for analysts and designers.

NOTES
1. Dimensions in feet
2. Not to scale

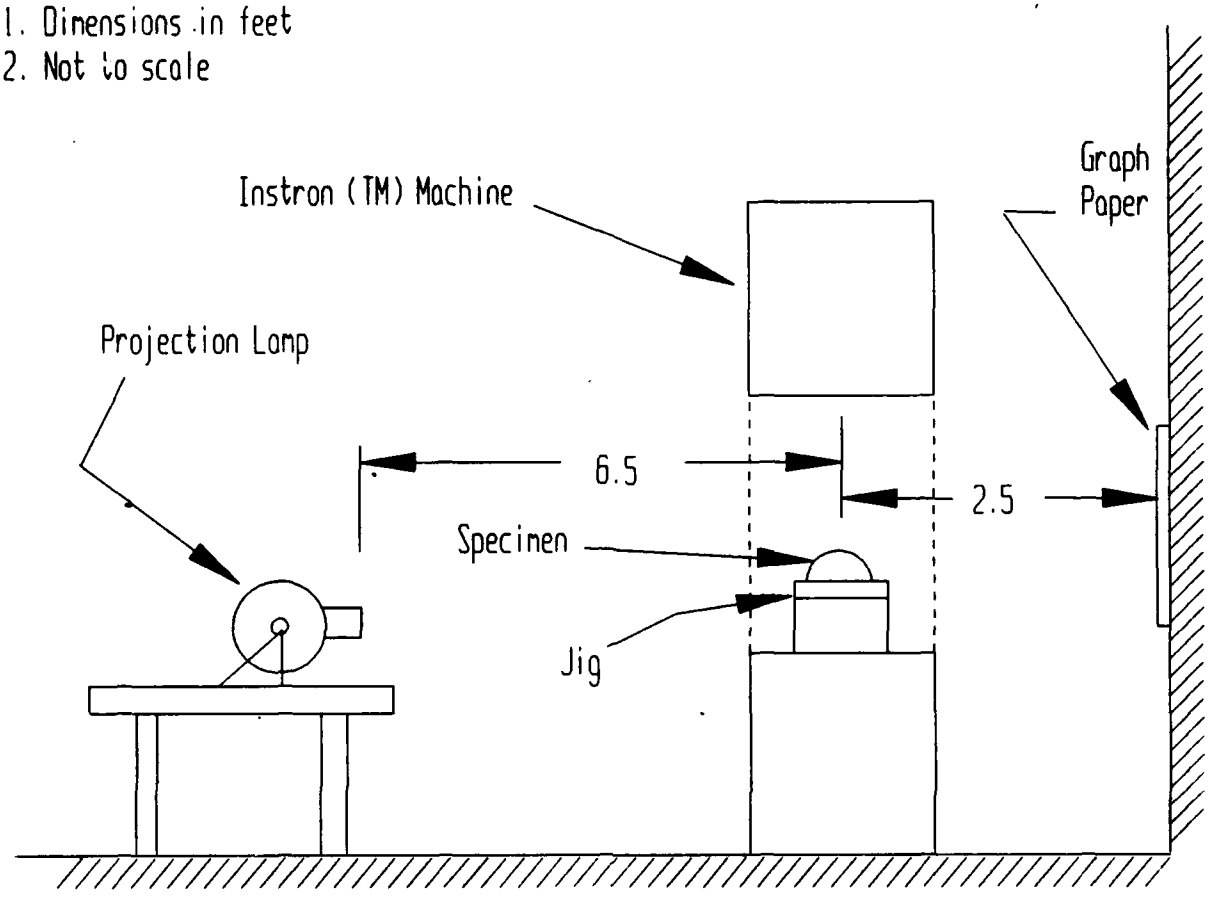

Figure 1. Layout of equipment.

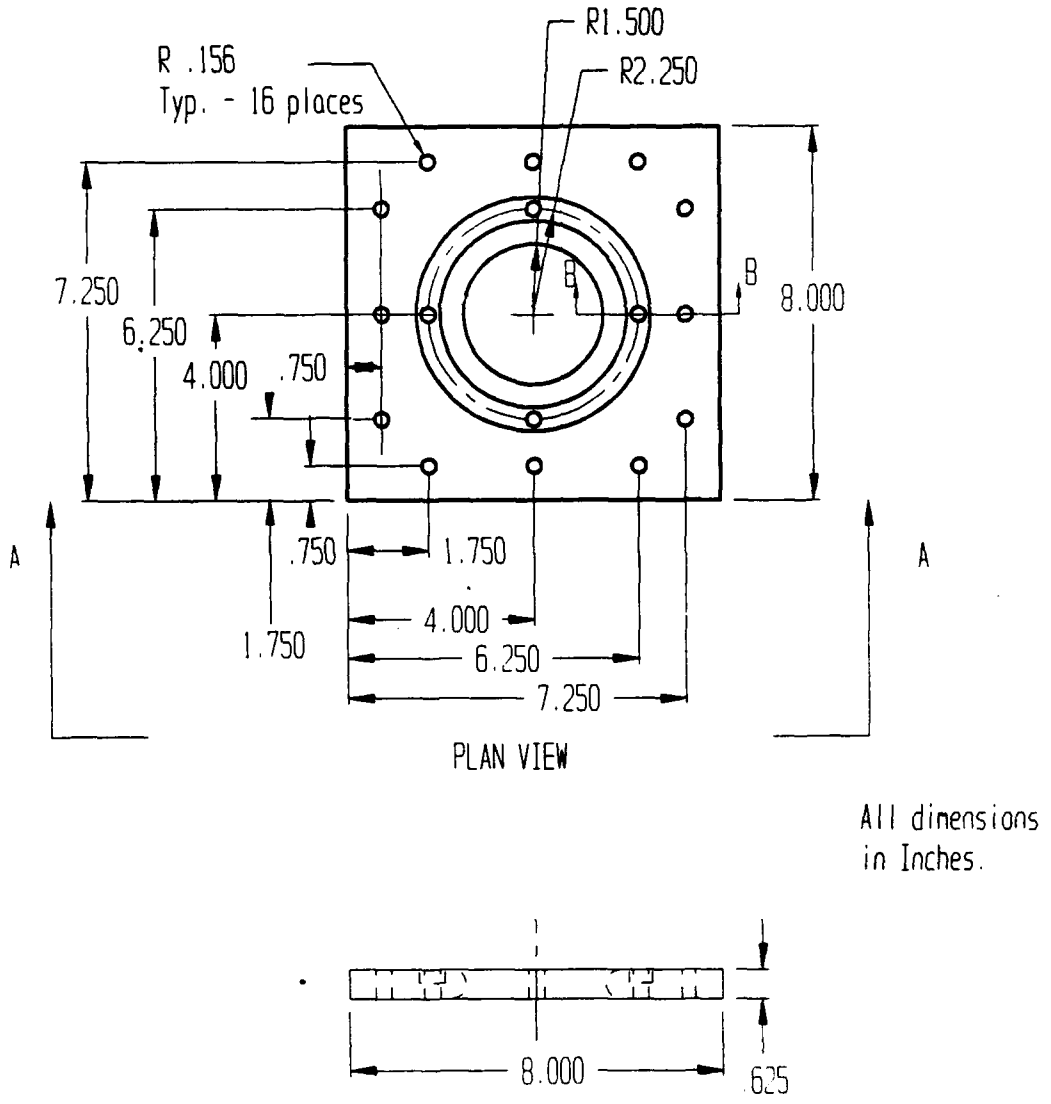

Figure 2. Details of jig's top plate design.

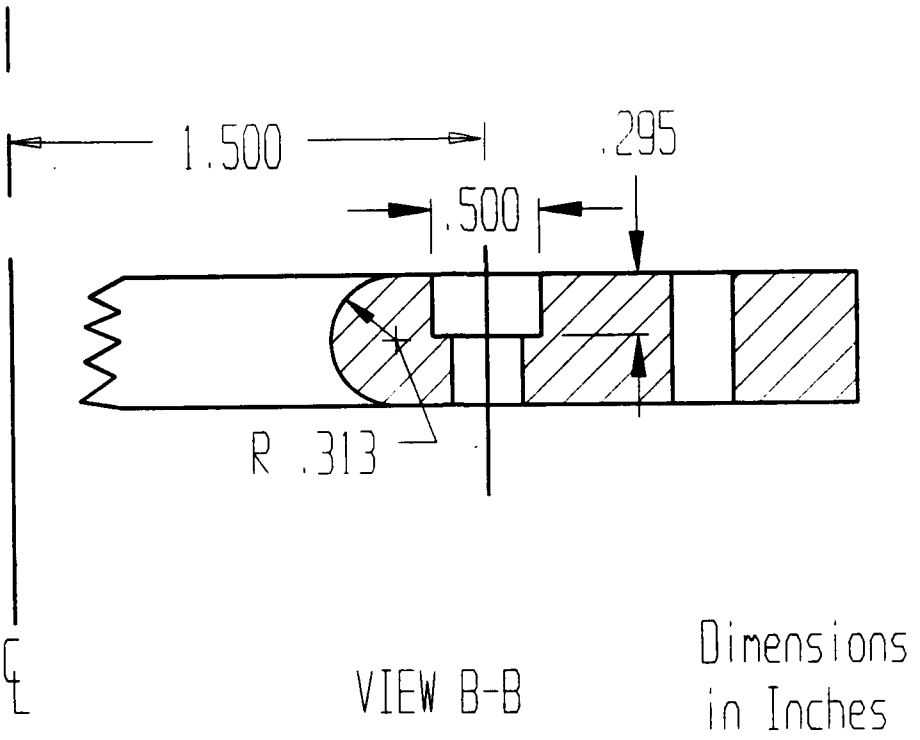

Figure 3. Cross section B-B of jig's top plate.

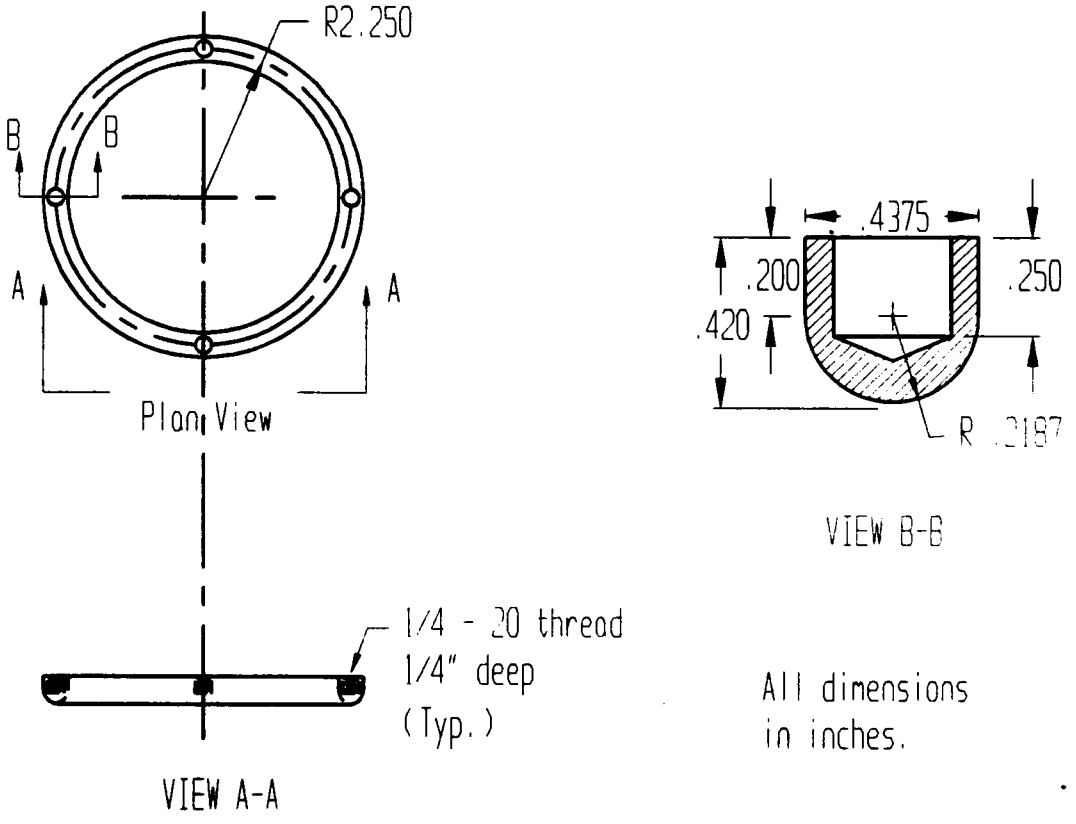

Figure 4. Jig's clamping ring.

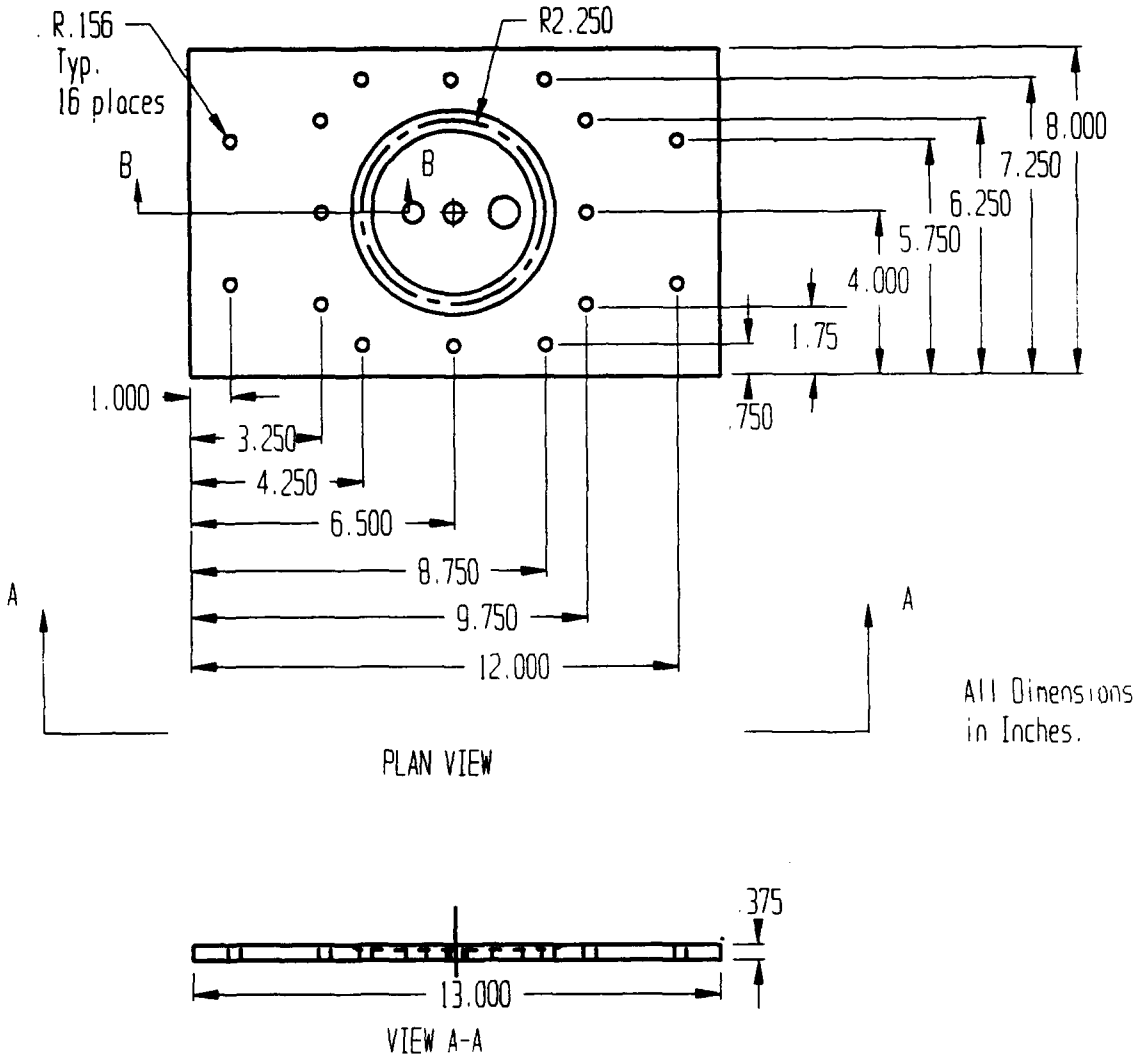

Figure 5. Bolt down holes of bottom plate.

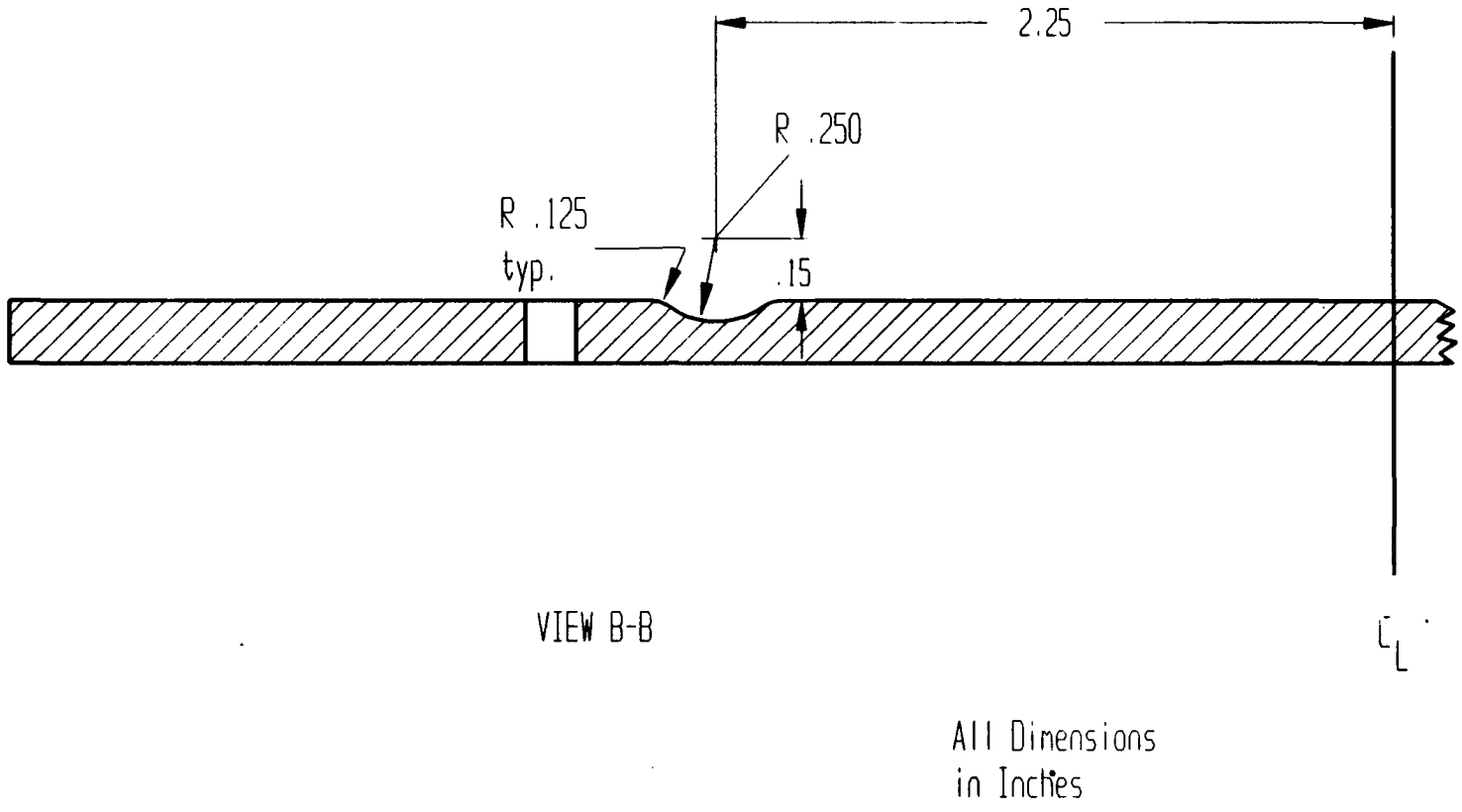

Figure 6. Jig's bottom plate view B-B.

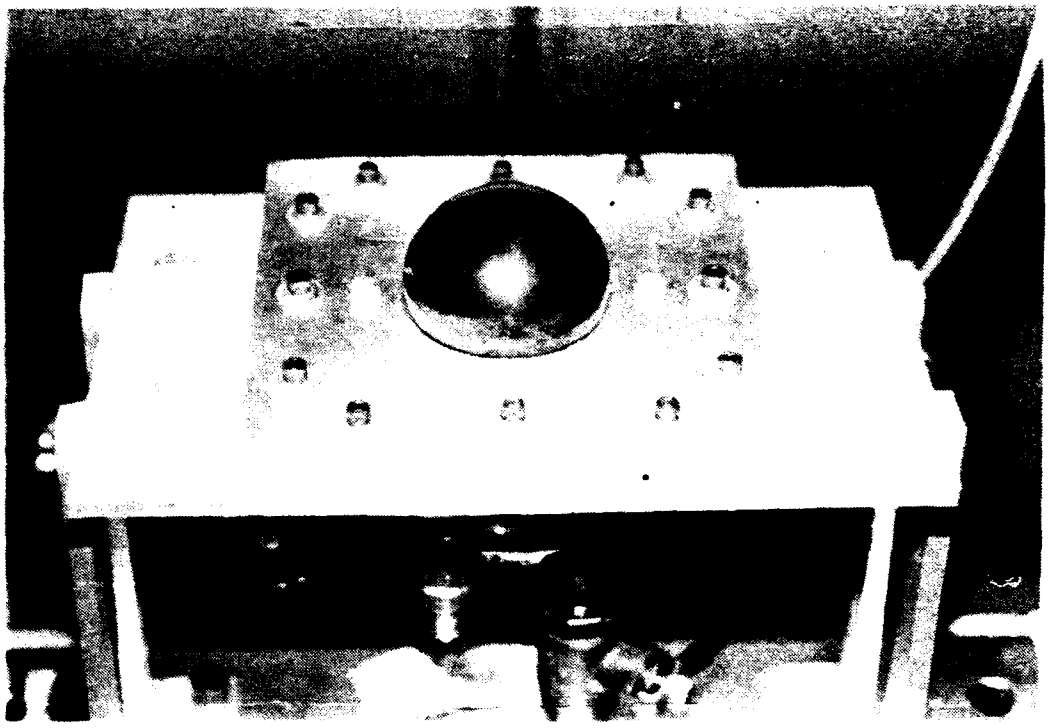

Figure 7. Inflated specimen in jig top plate and bottom plate - overview.

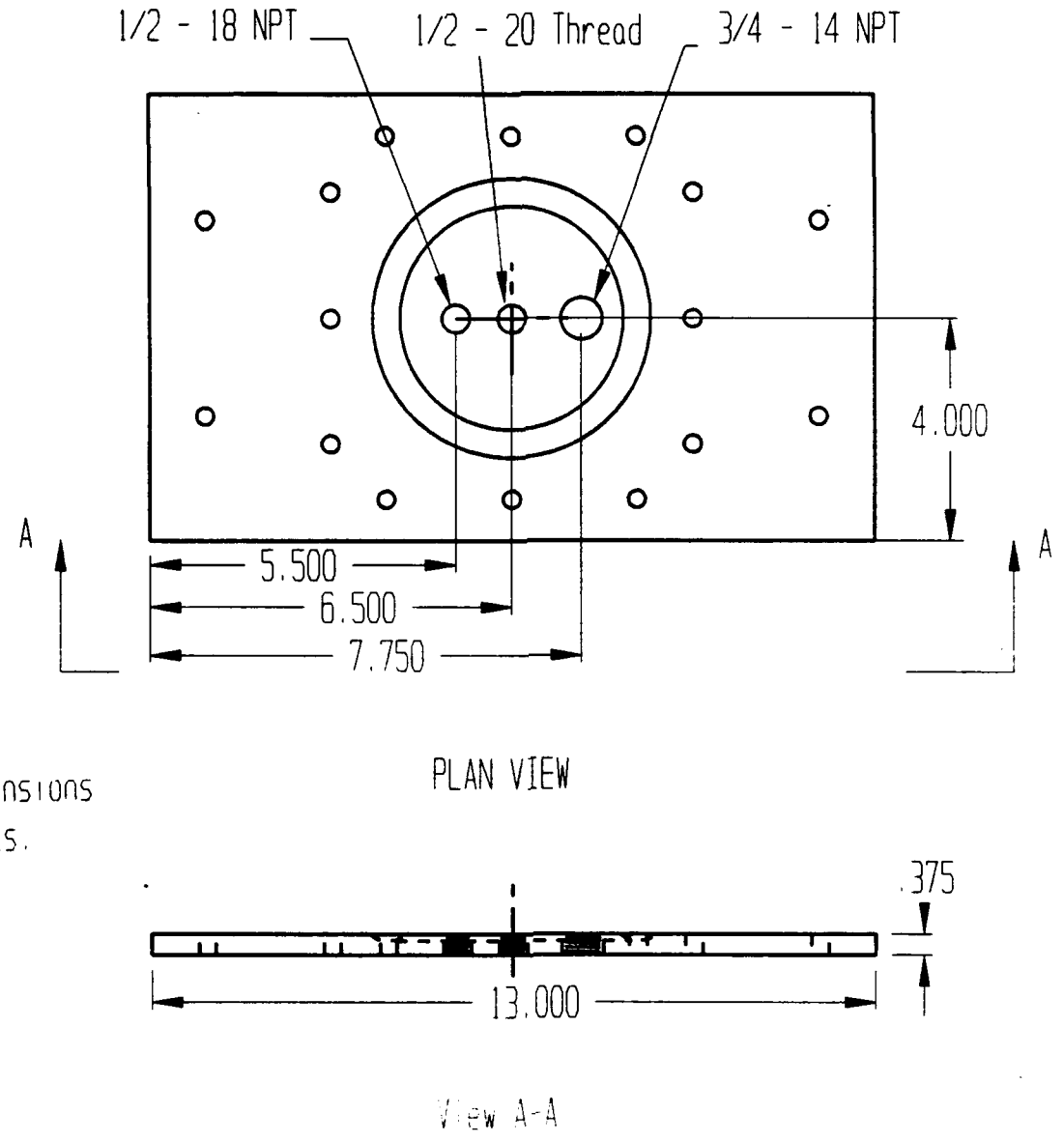

Figure 8. Jig's bottom plate.

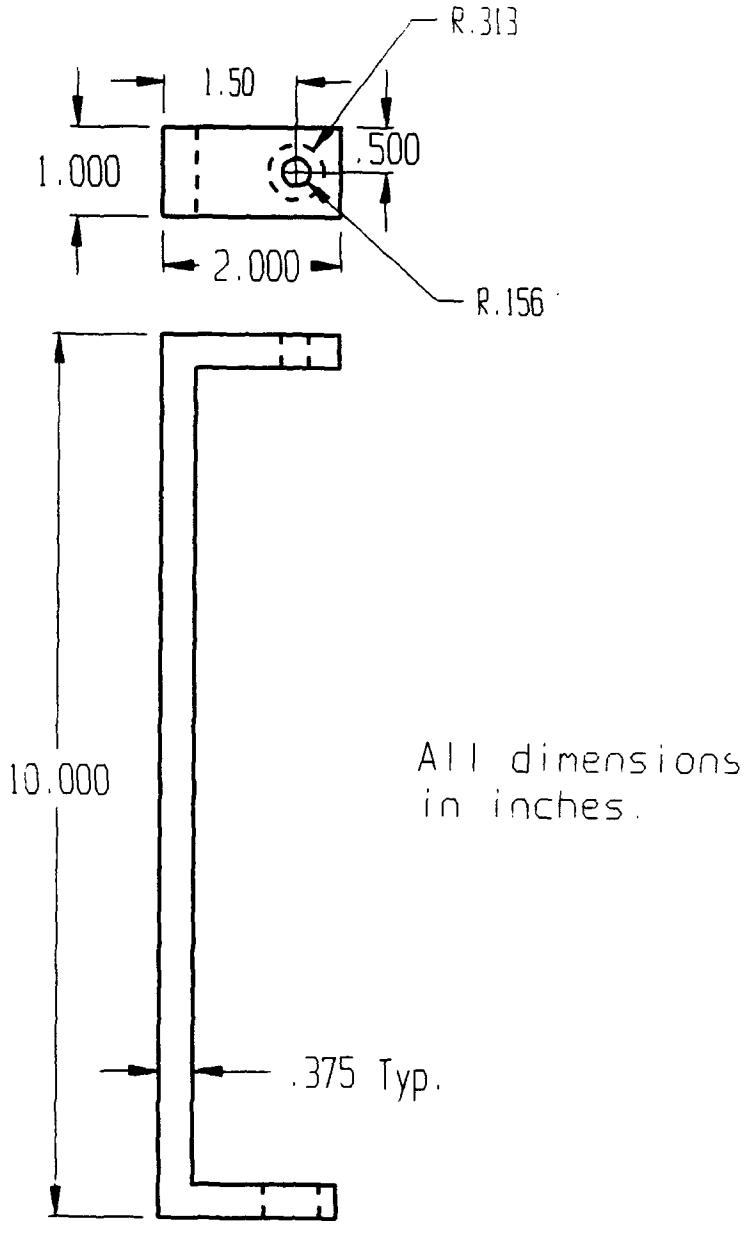

Figure 9. Jig fixture support.

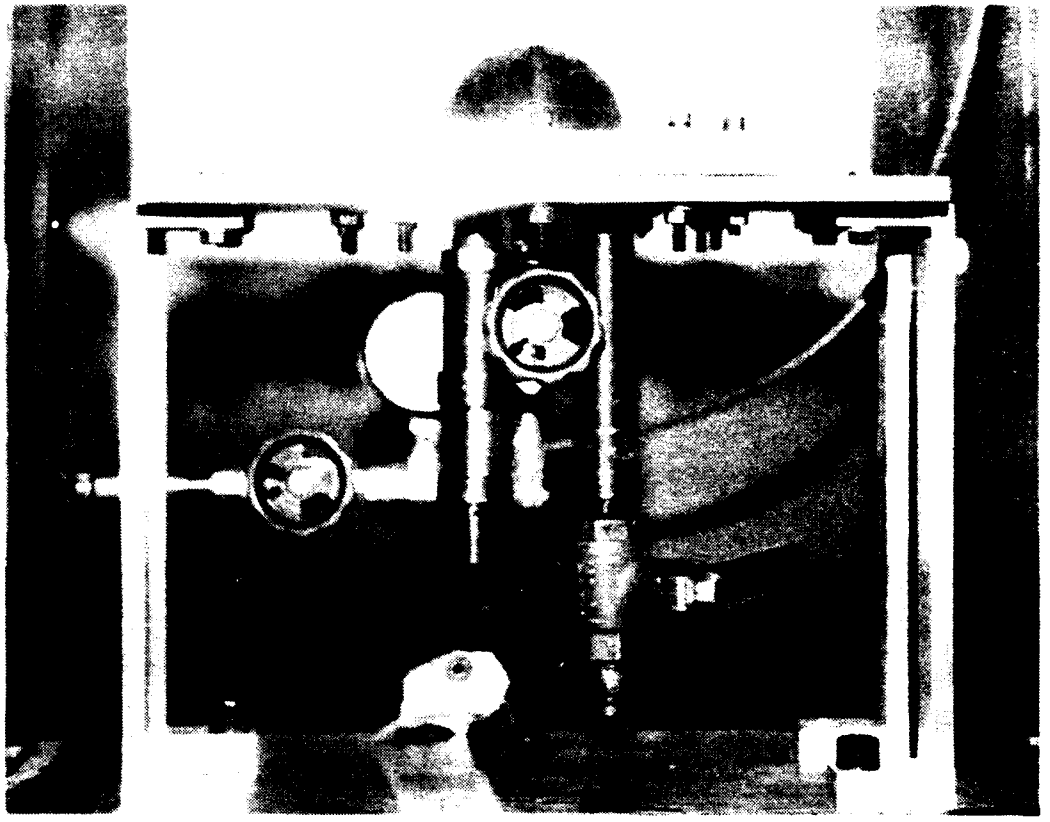

Figure 10. Inflated specimen in jig with air regulating system and fixture support - sideview.

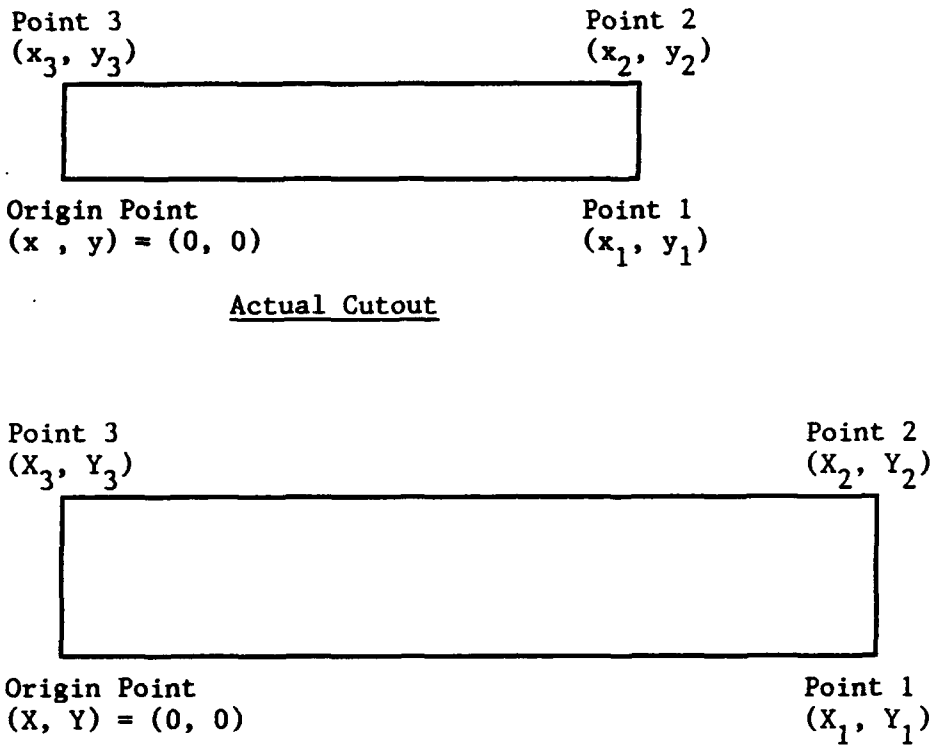

Figure 11. Example of a rectangular specimen used to calibrate mapping function.

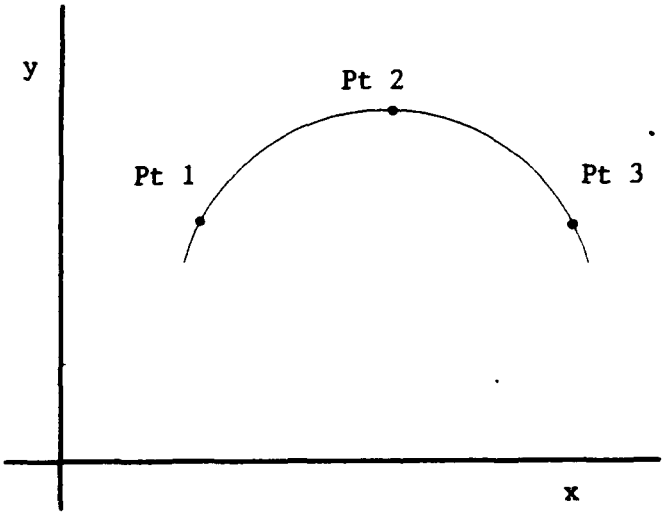

Figure 12. Marked points of specimen's image on graph paper.

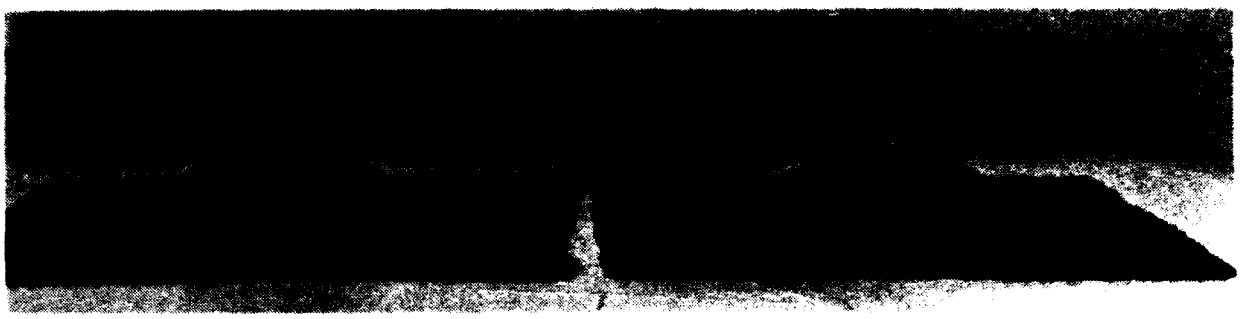

(a) (b)

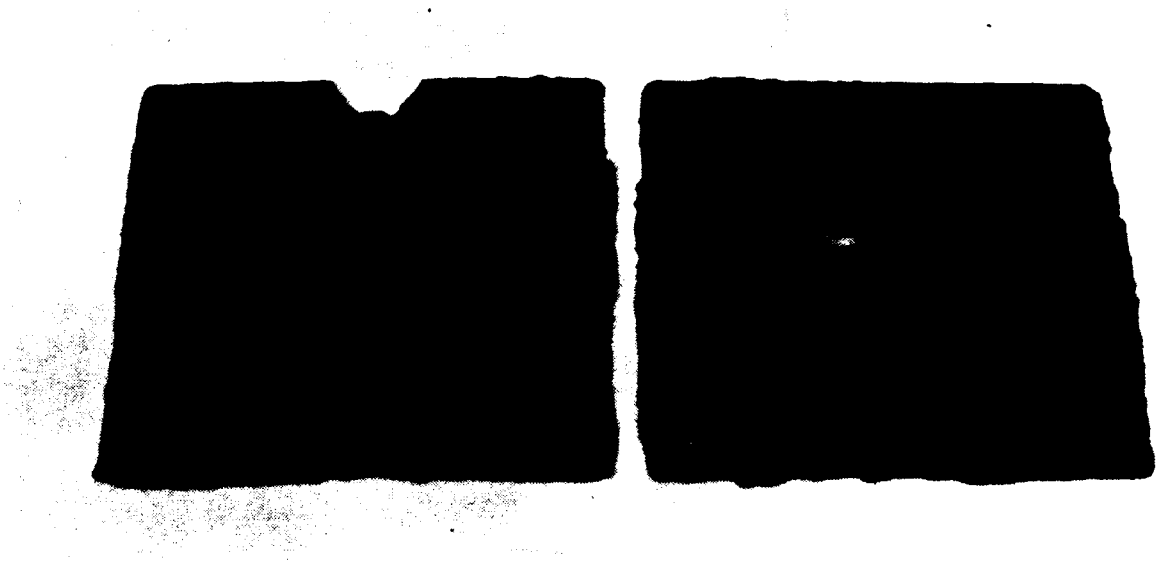

(a) (b)

Figure 13. Relaxed deformed specimens: (a) cycled, (b) failed.

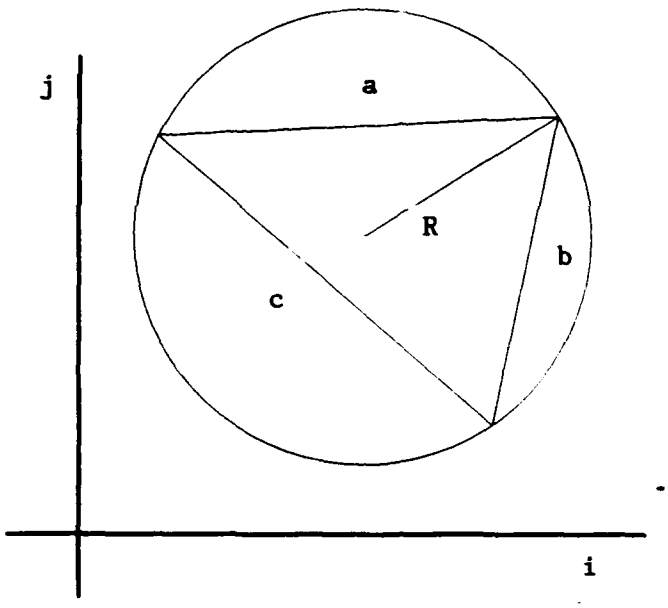

Figure 14. Geometry for finding radius of curvature.

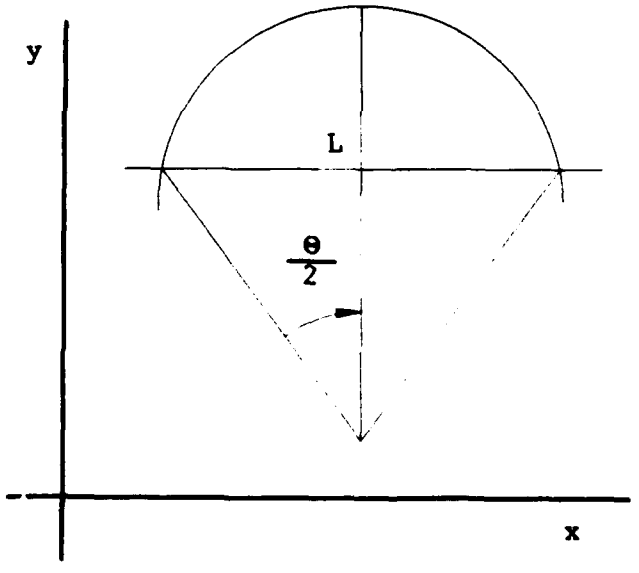

Figure 15. Geometry for and calculation of arc length and sector angle.

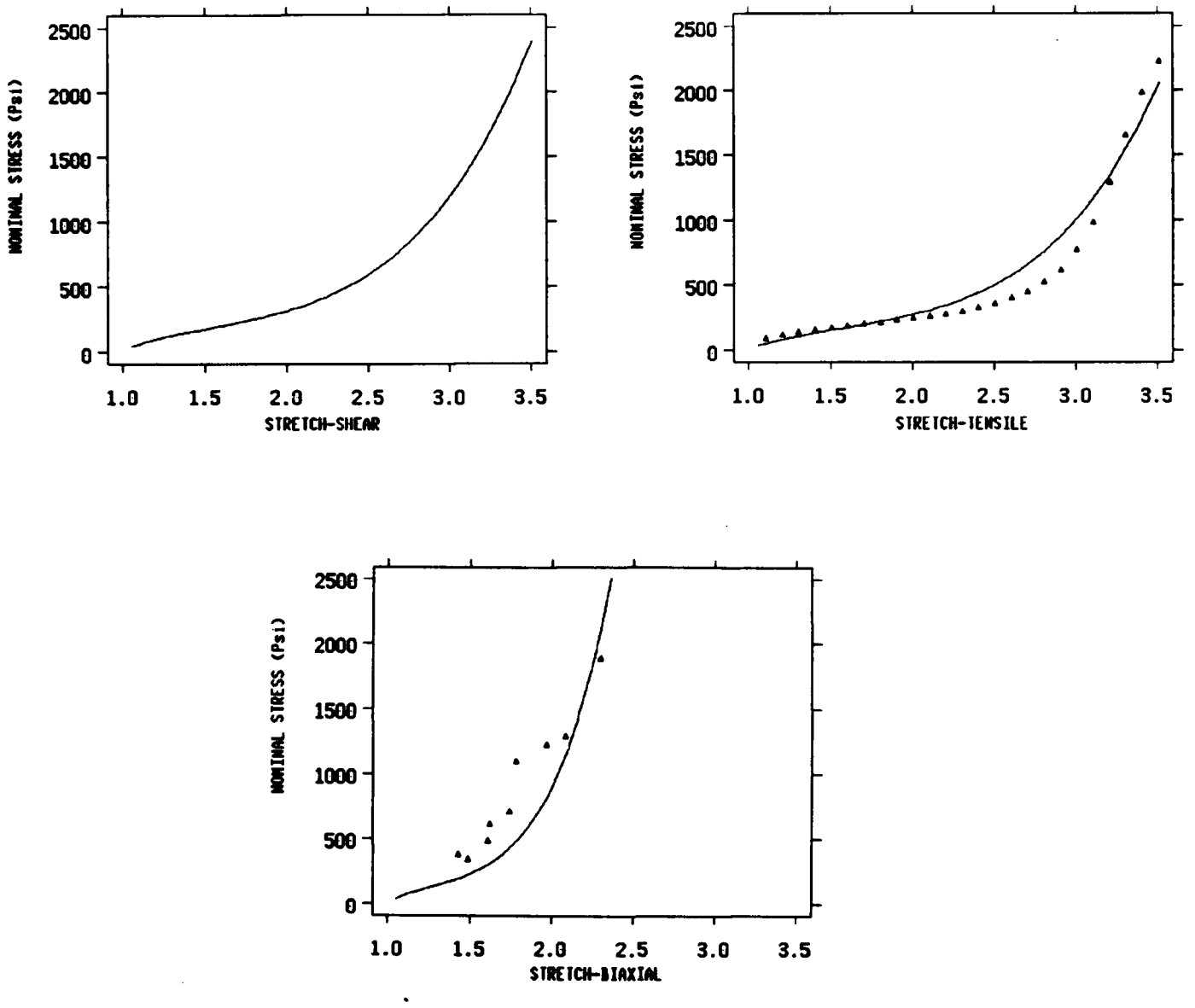

Figure 16. Lease squares fit of inflation data from test #1 and constant tension data. Experimental data represented by triangular points.

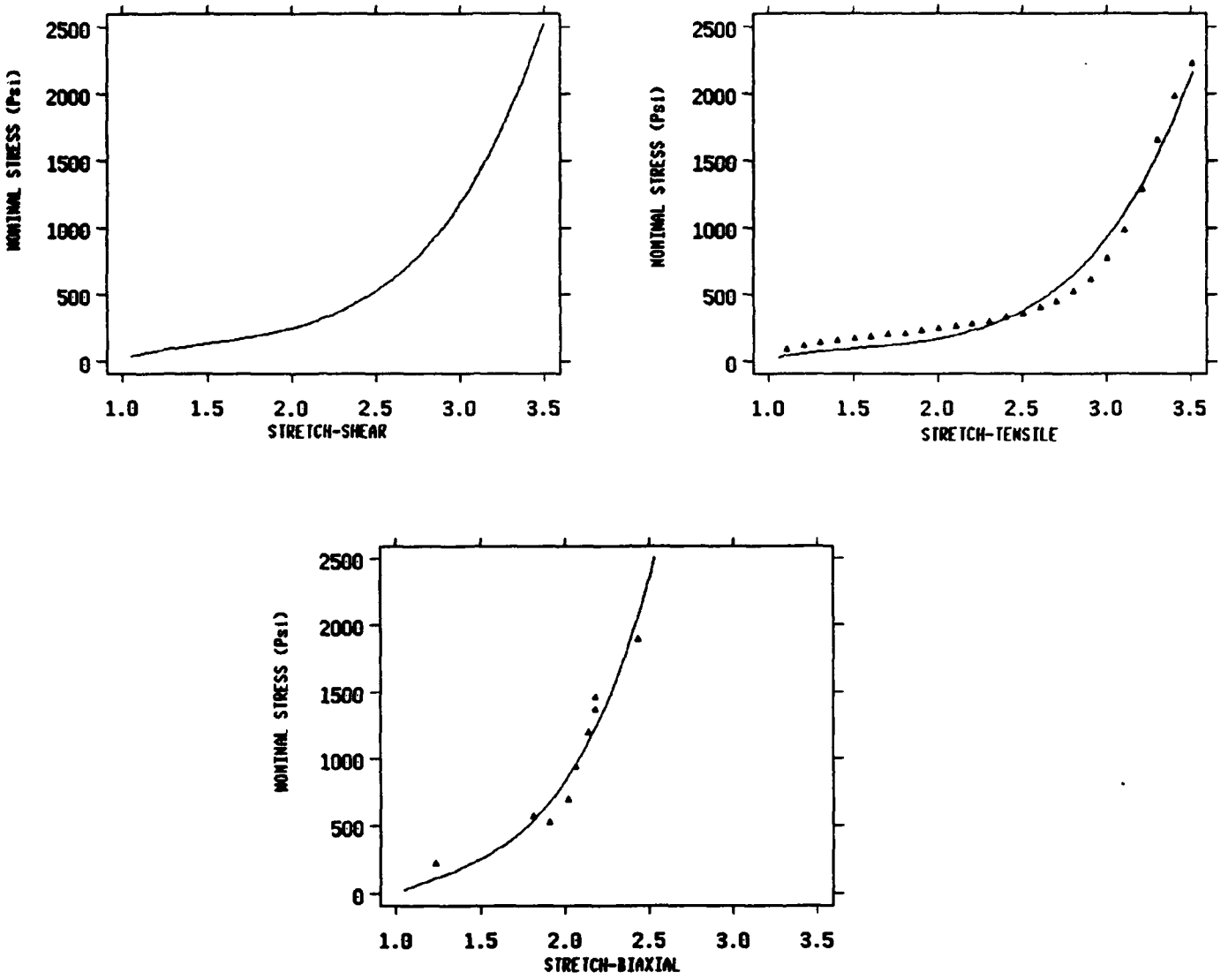

Figure 17. Least squares fit of inflation data from test #2 and constant tension data. Experimental data represented by triangular points.

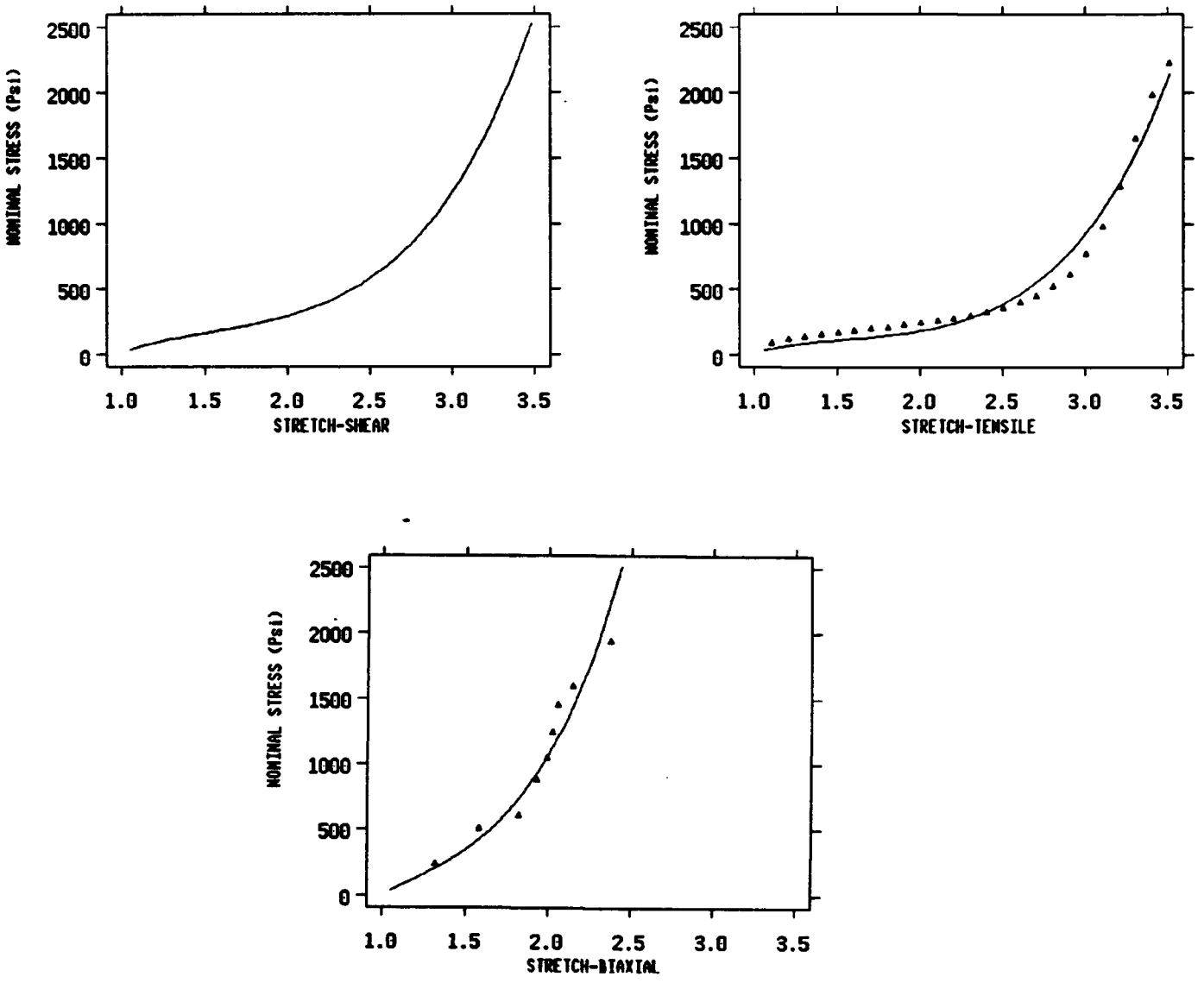

Figure 18. Least squares fit of inflation data from test #3 and constant tension data. Experimental data represented by triangular points.

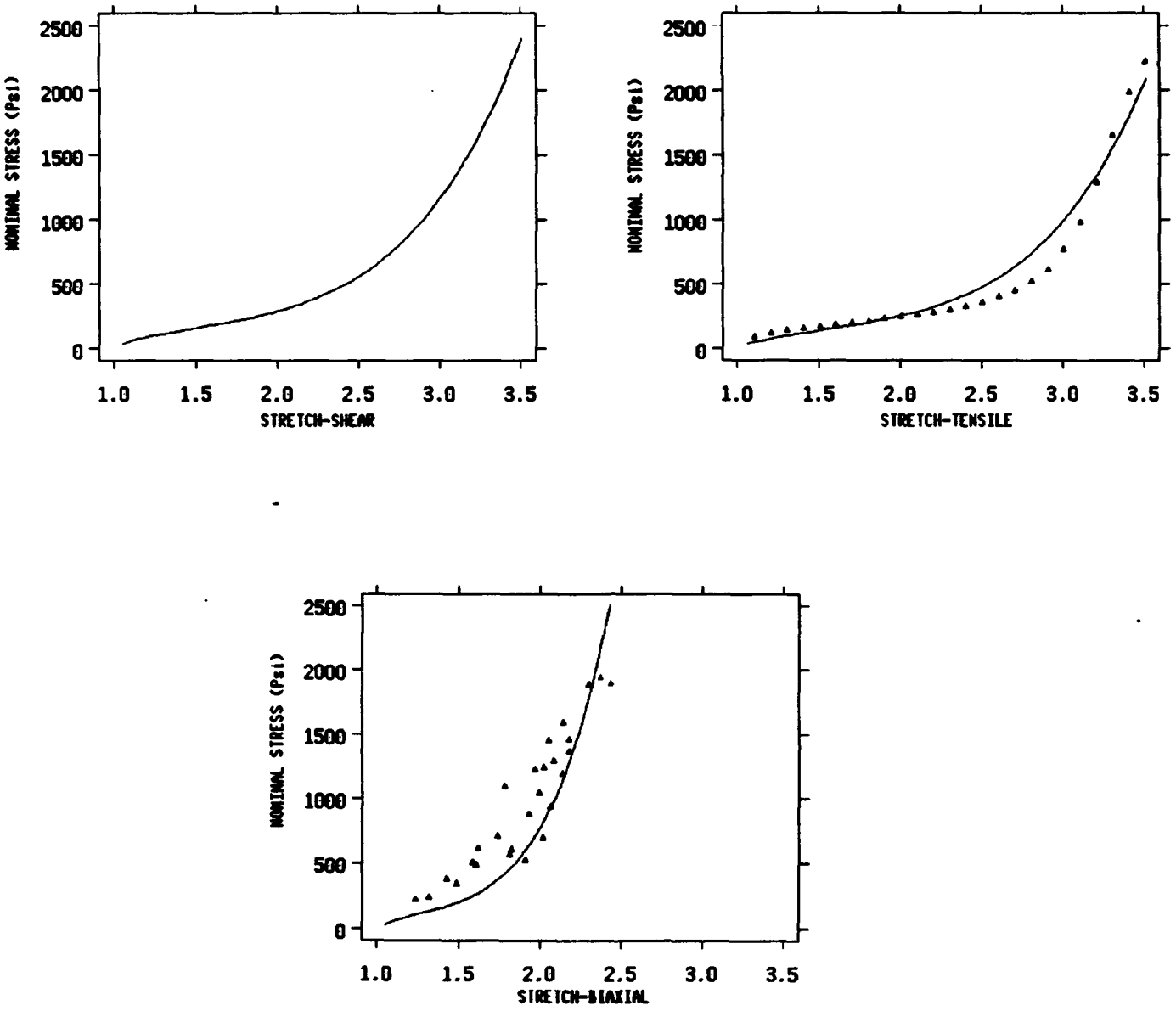

Figure 19. Least squares fit of inflation data from three equibiaxial tests and constant tension data. Experimental data represented by triangular points.

Table 1. COMPONENTS IN TP-14AX CARBON BLACK RUBBER

Natural Rubber	35.0
SBR - 1500	35.0
Takatene 220	30.0
Zinc Oxide	3.0
Stearic Acid	1.5
N - 220 Black	30.0
Sunolite 100	1.5
Sundex 790	4.0
Agerite Resin D	2.0
Santoflex 13	3.0
Sulfur	1.3
Santocure IPS, DIBS	3.2
Santogard PVI	0.2

Table 2. MEASURED POINTS FROM CUTOUT VERSUS MEASURED POINTS FROM CUTOUT IMAGE

		Actual Point	Image Point
Specimen #1	point 1	(3.7730,0.0000)	(5.2070,0.0000)
	point 2	(3.6400,1.0230)	(5.1810,1.3400)
	point 3	(0.0000,1.0220)	(0.0000,1.3410)
Specimen #2	point 1	(3.2800,0.0000)	(4.6120,0.0000)
	point 2	(3.2650,2.0330)	(4.5690,2.7260)
	point 3	(0.0000,2.0700)	(0.0000,2.7610)
Specimen #3	point 1	(4.2140,0.0000)	(5.8030,0.0000)
	point 2	(4.2380,2.1660)	(5.8320,2.8940)
	point 3	(0.0000,2.1650)	(0.0000,2.9060)

Table 3. COMPUTED AND ACTUAL LOCATIONS OF THE CORNERS OF RECTANGULAR CUTOUTS USED FOR CALIBRATING MAPPING FUNCTION

		computed location (inches)	actual location (inches)
Specimen #1	point 1	(3.7430, 0.0033)	(3.7730, 0.0000)
	point 2	(3.7235, 1.0052)	(3.6400, 1.0230)
	point 3	(-0.0157, 1,0210)	(0.0000, 1.0220)
	origin	(0.0000, 0.0000)	(0.0000, 0.0000)
Specimen #2	point 1	(3.3119, 0.0071)	(3.2800, 0.0000)
	point 2	(3.2829, 2.0409)	(3.2650, 2.0330)
	point 3	(-0.0011, 2.0640)	(0.0000, 2.0700)
	origin	(0.0000, 0.0000)	(0.0000, 0.0000)
Specimen #3	point 1	(4.1748, -0.0000)	(4.2140, 0.0000)
	point 2	(4.1905, 2.1675)	(4.2380, 2.1660)
	point 3	(0.0004, 2.1705)	(0.0000, 2.1650)
	origin	(0.0000, 0.0000)	(0.0000, 0.0000)

Table 4a. IMAGE POINTS TAKEN FROM GRAPH PAPER FOR EACH PRESSURE, SPECIMEN #1

P psi	Point # 1 (inches)	Point # 2 (inches)	Point # 3 (inches)
0	(0.095, 1.180)	(0.810, 1.360)	(1.500, 1.200)
17	(1.240, 1.500)	(2.230, 1.790)	(3.230, 1.570)
14	(1.200, 1.570)	(2.230, 1.870)	(3.280, 1.650)
18	(1.050, 1.950)	(2.210, 2.300)	(3.280, 2.050)
21	(1.050, 2.200)	(2.210, 2.510)	(3.320, 2.250)
21	(0.910, 2.300)	(2.210, 2.650)	(3.350, 2.390)
30	(0.870, 2.530)	(2.200, 2.920)	(3.380, 2.690)
31	(0.750, 2.650)	(2.200, 3.100)	(3.470, 2.800)
32	(0.690, 2.800)	(2.190, 3.300)	(3.520, 2.950)
37	(0.530, 3.350)	(2.180, 3.880)	(3.680, 3.500)

Table 4b. COMPUTED SHAPE OF SPECIMEN #1 FOR EACH PRESSURE

P psi	Point # 1 (inches)	Point # 2 (inches)	Point # 3 (inches)
0	(0.051, 0.902)	(0.569, 1.033)	(1.066, 0.913)
17	(0.880, 1.135)	(1.596, 1.347)	(2.316, 1.182)
14	(0.852, 1.186)	(1.597, 1.406)	(2.353, 1.241)
18	(0.747, 1.467)	(1.585, 1.724)	(2.354, 1.538)
21	(0.749, 1.651)	(1.586, 1.880)	(2.383, 1.687)
21	(0.649, 1.725)	(1.587, 1.983)	(2.406, 1.791)
30	(0.622, 1.894)	(1.581, 2.183)	(2.428, 2.013)
31	(0.537, 1.983)	(1.582, 2.316)	(2.493, 2.095)
32	(0.495, 2.093)	(1.576, 2.464)	(2.529, 2.207)
37	(0.385, 2.498)	(1.572, 2.894)	(2.646, 2.616)

Table 5a. IMAGE POINTS TAKEN FROM GRAPH PAPER FOR EACH PRESSURE, SPECIMEN #2

P psi	Point # 1 (inches)	Point # 2 (inches)	Point # 3 (inches)
0	(0.850, 1.080)	(1.550, 1.260)	(2.470, 1.020)
9.5	(1.620, 1.000)	(2.500, 1.200)	(3.670, 0.950)
18	(1.320, 1.720)	(2.500, 2.110)	(4.080, 1.550)
17	(1.300, 1.950)	(2.500, 2.390)	(4.090, 1.750)
20	(1.180, 2.150)	(2.510, 2.630)	(4.150, 1.990)
24	(1.070, 2.300)	(2.510, 2.800)	(4.180, 2.200)
29	(1.050, 2.520)	(2.500, 3.000)	(4.250, 2.320)
31	(0.980, 2.640)	(2.500, 3.150)	(4.280, 2.500)
33	(0.910, 2.750)	(2.450, 3.310)	(4.210, 2.720)
38	(0.830, 3.080)	(2.510, 3.700)	(4.400, 2.960)

Table 5b. COMPUTED SHAPE OF SPECIMEN #2 FOR EACH PRESSURE

P psi	Point # 1 (inches)	Point # 2 (inches)	Point # 3 (inches)
0	(0.596, 0.826)	(1.102, 0.957)	(1.765, 0.776)
9.5	(1.151, 0.764)	(1.788, 0.909)	(2.632, 0.720)
18	(0.940, 1.297)	(1.792, 1.583)	(2.929, 1.165)
17	(0.927, 1.467)	(1.794, 1.791)	(2.937, 1.314)
20	(0.842, 1.614)	(1.802, 1.969)	(2.980, 1.492)
24	(0.764, 1.725)	(1.803, 2.095)	(3.002, 1.649)
29	(0.752, 1.887)	(1.797, 2.243)	(3.053, 1.738)
31	(0.702, 1.975)	(1.798, 2.354)	(3.075, 1.872)
33	(0.653, 2.056)	(1.763, 2.472)	(3.025, 2.036)
38	(0.598, 2.300)	(1.808, 2.761)	(3.162, 2.215)

Table 6a. IMAGE POINTS TAKEN FROM GRAPH PAPER FOR EACH PRESSURE, SPECIMEN #3

P psi	Point # 1 (inches)	Point # 2 (inches)	Point # 3 (inches)
0	(-0.545, 0.882)	(0.000, 0.953)	(0.699, 0.858)
13	(-0.658, 0.604)	(0.000, 0.712)	(0.938, 0.492)
17	(-0.785, 1.217)	(0.000, 1.312)	(1.154, 1.047)
22	(-0.902, 1.624)	(0.000, 1.817)	(1.253, 1.457)
27	(-0.949, 1.860)	(0.000, 2.036)	(1.352, 1.645)
32	(-0.921, 2.023)	(0.000, 2.208)	(1.426, 1.778)
35.5	(-0.979, 2.157)	(0.057, 2.349)	(1.421, 1.938)
40	(-0.964, 2.325)	(0.057, 2.505)	(1.475, 2.071)
42.5	(-0.991, 2.509)	(0.073, 2.699)	(1.535, 2.217)
44	(-1.081, 2.957)	(0.131, 3.125)	(1.697, 2.507)

Table 6b. COMPUTED SHAPE OF SPECIMEN #3 FOR EACH PRESSURE

P psi	Point # 1 (inches)	Point # 2 (inches)	Point # 3 (inches)
0	(-0.414, 0.686)	(-0.020, 0.736)	(0.485, 0.663)
13	(-0.499, 0.482)	(-0.022, 0.559)	(0.655, 0.393)
17	(-0.583, 0.932)	(-0.016, 1.000)	(0.815, 0.801)
22	(-0.663, 1.231)	(-0.011, 1.371)	(0.889, 1.103)
27	(-0.694, 1.403)	(-0.009, 1.531)	(0.962, 1.241)
32	(-0.672, 1.523)	(-0.007, 1.658)	(1.017, 1.339)
35.5	(-0.713, 1.621)	(0.036, 1.761)	(1.014, 1.457)
40	(-0.699, 1.744)	(0.037, 1.876)	(1.054, 1.556)
42.5	(-0.717, 1.879)	(0.051, 2.018)	(1.098, 1.664)
44	(-0.776, 2.206)	(0.097, 2.332)	(1.217, 1.878)

Table 7. CALCULATED VALUES OF RADIUS, ANGLE, AND ARC LENGTH FOR SPECIMEN #1

P psi	Radius (inches)	Angle (radians)	Arc Length (inches)
0	1.091	.999	1.090
17	1.462	1.065	1.557
14	1.561	1.039	1.621
18	1.576	1.115	1.757
21	1.692	1.044	1.767
21	1.833	1.035	1.897
30	1.922	1.012	1.945
31	1.884	1.140	2.148
32	1.819	1.251	2.275
37	2.082	1.204	2.508

Table 8. CALCULATED VALUES OF RADIUS, ANGLE, AND ARC LENGTH FOR SPECIMEN #2

P psi	Radius (inches)	Angle (radians)	Arc Length (inches)
0	1.183	1.075	1.271
9.5	1.722	0.913	1.572
18	1.591	1.450	2.308
17	1.473	1.650	2.430
20	1.592	1.609	2.561
24	1.743	1.505	2.623
29	1.769	1.535	2.716
31	1.858	1.493	2.774
33	1.861	1.488	2.769
38	1.885	1.638	3.088

Table 9. CALCULATED VALUES OF RADIUS, ANGLE, AND ARC LENGTH FOR SPECIMEN #3

P psi	Radius (inches)	Angle (radians)	Arc Length (inches)
0	1.681	0.546	0.919
13	1.485	0.816	1.212
17	2.028	0.717	1.454
22	1.621	1.036	1.679
27	1.819	0.977	1.779
32	1.765	1.037	1.830
35.5	1.856	1.002	1.860
40	1.901	0.993	1.887
42.5	1.883	1.046	1.970
44	2.006	1.087	2.181

Table 10. STRETCH-STRESS DATA FOR TEST SPECIMENS 1, 2, AND 3 FOR INFLATION TEST AND TENSILE DATA

INFLATION DATA
Specimen No 1

λ	σ(psi)
1.00	0.00
1.43	377.77
1.49	345.70
1.61	486.37
1.62	612.97
1.74	712.75
1.78	1094.86
1.97	1224.18
2.09	1292.31
2.30	1885.97

INFLATION DATA
Specimen No 2

λ	σ(psi)
1.00	0.00
1.24	219.96
1.82	565.41
1.91	520.48
2.02	697.63
2.06	938.39
2.14	1191.90
2.18	1367.09
2.17	1454.38
2.43	1892.76

INFLATION DATA
Specimen No 3

λ	σ(psi)
1.00	0.00
1.32	235.96
1.58	505.41
1.83	603.70
1.94	880.69
1.99	1041.55
2.02	1235.04
2.05	1445.98
2.14	1589.02
2.37	1840.40

TENSION DATA

λ	σ(psi)
1.00	0.00
1.10	92.98
1.20	130.75
1.30	159.81
1.40	180.15
1.50	197.58
1.60	215.02
1.70	226.64
1.80	246.98
1.90	261.51
2.00	284.75
2.10	305.09
2.20	325.43
2.30	348.68
2.40	377.73
2.50	418.41
2.60	459.09
2.70	508.48
2.80	581.13
2.90	668.29
3.00	799.05
3.10	958.86
3.20	1191.31
3.30	1464.44
3.40	1816.02
3.50	2033.94

Table 11. MATERIAL CONSTANTS FOUND FOR LEAST SQUARE ERROR OF THE DATA FROM THE THREE TESTS TOGETHER WITH THE REFERENCED TENSION DATA

TEST #1		TEST #2		TEST #3	
C_{10}	81.556	C_{10}	38.882	C_{10}	34.560
C_{01}	0.000	C_{01}	27.931	C_{01}	44.769
C_{11}	0.000	C_{11}	0.000	C_{11}	0.000
C_{20}	0.000	C_{20}	0.000	C_{20}	0.000
C_{02}	0.977	C_{02}	0.034	C_{02}	0.000
C_{21}	0.000	C_{21}	0.000	C_{21}	0.000
C_{12}	0.000	C_{12}	0.000	C_{12}	0.000
C_{30}	0.650	C_{30}	0.826	C_{30}	0.816
C_{03}	0.000	C_{03}	0.000	C_{03}	0.000

APPENDIX

Properties of TO-14AX

Original

- Tensile, PSI 2850
- 200% Mod., PSI 1450
- Elong., % 340
- Hardness Shore A 73
- Bashore, Rebound, % 35
- SP. Gravity 1.1294
- Cure, Minutes at F 40/310

Abrasion

- Taber, G/1000 Cycles 0.330
- Pico at Room Temperature 222

Tear Strength, Die C, Lb/In 409

- Unaged 243
- 10 Minutes at 250°F 157
- 4 Hours at 250°F 156
- 4 Hours at 300°F 64

Tear Strength, Die C, Lb/In

Goodrich Cutting and Clipping

- Diameter Loss, Inches 0.158
- Weight Loss, Gram 2.239

Brittleness at -40°F . . . . . PASS

Ross Flex - 250,000 Cycles

- Unaged - (Crack Growth, %) 267
- Aged 70 Hours at 212°F
  - Growth % . . . . . FAIL
- Aged 20 Hours at 250°F
  - Growth % . . . . . FAIL

Mooney Viscometer

- ML 3 + 4 at 212°F 66
- T5 at 250°F 81

Dematha Flex

- Unaged, Growth Rate, Mil/Min 36
- 212°F, Growth Rate, Mil/Min 171
- 250°F, Growth Rate, Mil/Min 333
- Crack Initiation, Cycles x 1000 . . . . . 4.5

Goodrich Flex at 50°C

- Temperature Rise External, °C 35
- Static Comp, % 15
- Dynamic Comp, % 11
- Permanent Set, % 5
- Blow Out Time, Minutes 26

Compressibility

- Unaged
  - 10%, Lb 117
  - 20%, Lb 223
  - 40%, Lb 517
- 20 Hours at 250°F
  - 10%, Lb 80
  - 20%, Lb 197
  - 40%, Lb 515

Heat Resistance

- Oven Aged 20 Hours at 212°F
  - Elong. Ret., % 57
  - Ten Ret., % 81
- Oven Aged 20 Hours at 250°F
  - Elong. Ret., % 35
  - Ten Ret., % 66

DISTRIBUTION LIST

No. of Copies	To
1	Office of the Under Secretary of Defense for Research and Engineering, The Pentagon, Washington, DC 20301
	Commander, U.S. Army Laboratory Command, 2800 Powder Mill Road, Adelphi, MD 20783-1145
1	ATTN: AMSLC-IM-TL
1	AMSLC-CT
	Commander, Defense Technical Information Center, Cameron Station, Building 5, 5010 Duke Street, Alexandria, VA 22304-6145
2	ATTN: DTIC-FDAC
1	MIAC/CINDAS, Purdue University, 2595 Yeager Road, West Lafayette, IN 47905
	Commander, Army Research Office, P.O. Box 12211, Research Triangle Park, NC 27709-2211
1	ATTN: Information Processing Office
	Commander, U.S. Army Materiel Command, 5001 Eisenhower Avenue, Alexandria, VA 22333
1	ATTN: AMCSCI
	Commander, U.S. Army Missile Command, Redstone Scientific Information Center, Redstone Arsenal, AL 35898-5241
1	ATTN: AMSMI-RD-CS-R/Doc
1	AMSMI-RLM
	Commander, U.S. Army Natick Research, Development and Engineering Center, Natick, MA 01760-5010
1	ATTN: Technical Library
	Commander, U.S. Army Tank-Automotive Command, Warren, MI 48397-5000
1	ATTN: AMSTA-ZSK
1	AMSTA-TSL, Technical Library
	Director, U.S. Army Ballistic Research Laboratory, Aberdeen Proving Ground, MD 21005
1	ATTN: SLCBR-TSB-S (STINFO)
	Commander, Harry Diamond Laboratories, 2800 Powder Mill Road, Adelphi, MD 20783
1	ATTN: Technical Information Office
	Director, Benet Weapons Laboratory, LCWSL, USA AMCCOM, Watervliet, NY 12189
1	ATTN: AMSMC-LCB-TL
	Commander, U.S. Army Foreign Science and Technology Center, 220 7th Street, N.E., Charlottesville, VA 22901-5396
3	ATTN: AIFRTC, Applied Technologies Branch, Gerald Schlesinger
1	Plastics Technical Evaluation Center, (PLASTEC), ARDEC, Bldg. 355N, Picatinny Arsenal, NJ 07806-5000
	Commander, Naval Underwater Systems Center, Newport, RI 02841-5047
1	ATTN: Code 8333/Bldg. 1246, Laurent C. Bissonnette
	Commander, Naval Underwater Systems Center, New London, CT 06320-5594
1	ATTN: Code 44, Dr. Donald L. Cox
	Director, U.S. Army Materials Technology Laboratory, Watertown, MA 02172-0001
2	ATTN: SLCMT-TML
4	Authors

U.S. Army Materials Technology Laboratory
Watertown, Massachusetts 02172-0001
EQUIBIAXIAL TESTING OF TP-14AX CARBON BLACK RUBBER SHEETS -
Robert P. Bamberg, Ronald R. Aghababian, Christopher Cavallaro, and Arthur R. Johnson

Technical Report MTL TR 92-50, August 1992, 38 pp- illus-tables, D/A Project: 1L161102AH42

AD_____
UNCLASSIFIED
UNLIMITED DISTRIBUTION

Key Words

Elastomers
Inflation tests
Stress-stretch tests

The classical inflation test for thin rubber disks was used to obtain equibiaxial stress-stretch data for a carbon black filled rubber (TP-14AX). Details of the experimental setup, test procedure, measured data, and material constants obtained from the data are reported. A review of how to use the measured test data with tensile stress-stretch data to obtain the material constants is presented. Complete results (data to material constants) for three test specimens are reported.

U.S. Army Materials Technology Laboratory
Watertown, Massachusetts 02172-0001
EQUIBIAXIAL TESTING OF TP-14AX CARBON BLACK RUBBER SHEETS -
Robert P. Bamberg, Ronald R. Aghababian, Christopher Cavallaro, and Arthur R. Johnson

Technical Report MTL TR 92-50, August 1992, 38 pp- illus-tables, D/A Project: 1L161102AH42

AD_____
UNCLASSIFIED
UNLIMITED DISTRIBUTION

Key Words

Elastomers
Inflation tests
Stress-stretch tests

The classical inflation test for thin rubber disks was used to obtain equibiaxial stress-stretch data for a carbon black filled rubber (TP-14AX). Details of the experimental setup, test procedure, measured data, and material constants obtained from the data are reported. A review of how to use the measured test data with tensile stress-stretch data to obtain the material constants is presented. Complete results (data to material constants) for three test specimens are reported.

U.S. Army Materials Technology Laboratory
Watertown, Massachusetts 02172-0001
EQUIBIAXIAL TESTING OF TP-14AX CARBON BLACK RUBBER SHEETS -
Robert P. Bamberg, Ronald R. Aghababian, Christopher Cavallaro, and Arthur R. Johnson

Technical Report MTL TR 92-50, August 1992, 38 pp- illus-tables, D/A Project: 1L161102AH42

AD_____
UNCLASSIFIED
UNLIMITED DISTRIBUTION

Key Words

Elastomers
Inflation tests
Stress-stretch tests

The classical inflation test for thin rubber disks was used to obtain equibiaxial stress-stretch data for a carbon black filled rubber (TP-14AX). Details of the experimental setup, test procedure, measured data, and material constants obtained from the data are reported. A review of how to use the measured test data with tensile stress-stretch data to obtain the material constants is presented. Complete results (data to material constants) for three test specimens are reported.

U.S. Army Materials Technology Laboratory
Watertown, Massachusetts 02172-0001
EQUIBIAXIAL TESTING OF TP-14AX CARBON BLACK RUBBER SHEETS -
Robert P. Bamberg, Ronald R. Aghababian, Christopher Cavallaro, and Arthur R. Johnson

Technical Report MTL TR 92-50, August 1992, 38 pp- illus-tables, D/A Project: 1L161102AH42

AD_____
UNCLASSIFIED
UNLIMITED DISTRIBUTION

Key Words

Elastomers
Inflation tests
Stress-stretch tests

The classical inflation test for thin rubber disks was used to obtain equibiaxial stress-stretch data for a carbon black filled rubber (TP-14AX). Details of the experimental setup, test procedure, measured data, and material constants obtained from the data are reported. A review of how to use the measured test data with tensile stress-stretch data to obtain the material constants is presented. Complete results (data to material constants) for three test specimens are reported.